



OPEN

Anterior pituitary gland T1 signal intensity is influenced by time delay after injection of gadodiamide

Carlo A. Mallio¹✉, Laura Messina¹, Marco Parillo¹, Gianguido Lo Vullo¹, Bruno Beomonte Zobel¹, Paul M. Parizel² & Carlo C. Quattrocchi¹

To test the hypothesis of washout from the anterior pituitary (AP) gland after serial injections of gadodiamide. We included 59 patients with history of at least 5 injections of gadodiamide. Values of mean signal intensity of the AP and of the central pons were measured on unenhanced sagittal T1-weighted images. AP-to-pons signal intensity ratios were calculated dividing the values of the AP by those of the pons. The measurements were performed using MR images acquired at four different time points including baseline (prior to any gadodiamide injection), minimum post-injection time delay, maximum post-injection time delay, and last available MR scans. Normalized ratios (i.e. ratios divided total volume of injected gadodiamide) were also calculated. To assess the difference between ratios, non-parametric Wilcoxon signed-rank test was applied. The correlations were tested with non-parametric Spearman correlation coefficient. A p-value < 0.05 was considered as statistically significant. A statistically significant increase of AP signal intensity was found by comparing the baseline scans with both the minimum time delay (p = 0.003) and maximum time delay scans (p = 0.005). We found significant higher normalized ratios for minimum post-injection time delay with respect to maximum post-injection time delay (p < 0.001). The normalized ratios demonstrated a statistically significant negative correlation with the post-injection time delay (r = - 0.31; p = 0.006). The findings of this study suggest that washout phenomena of retained/deposited gadolinium from the AP are influenced by the total injected volume and post-injection time delay.

The pituitary gland plays a key role in regulating body homeostasis by integrating external and paracrine/autocrine pathways¹. It is located into a small bony cavity called sella turcica and it has two anatomically and functionally distinct lobes, the anterior pituitary (AP) (or adenohypophysis) and the posterior pituitary (or neurohypophysis)¹.

Gadolinium is a heavy metal with strong paramagnetic properties that is administered to humans during contrast-enhanced MR imaging studies in the form of gadolinium-based contrast agents (GBCAs)^{2,3}.

Since 2014, T1 hyperintensity on unenhanced MRI images of some intracranial structures, including the dentate nucleus (DN) and the globus pallidus (GP), has been associated to multiple injections of GBCAs⁴⁻¹². This association was very strong for those GBCAs with a linear structure, that are known to have a lower thermodynamic and kinetic stability as compared to those with a macrocyclic structure^{13,14}.

The currently available scientific literature failed to demonstrate causal relationship between gadolinium deposition and clinical neurological and neuropsychological or MR imaging changes indicative of tissue disruption¹⁵⁻²¹. Moreover, preclinical animal as well as human autopsy studies showed no histological tissue changes associated to gadolinium deposition^{6,22,23}.

Recently, it has been reported an increased signal intensity of the AP on unenhanced T1-weighted images in patients who had undergone intravenous injections of gadodiamide, suggesting gadolinium deposition or

¹Unit of Diagnostic Imaging and Interventional Radiology, Departmental Faculty of Medicine and Surgery, Università Campus Bio-Medico di Roma, Via Alvaro del Portillo, 21, 00128 Rome, Italy. ²Department of Radiology, Antwerp University Hospital, Edegem, Belgium. ✉email: c.mallio@unicampus.it

long-term retention²⁴. After that, the presence of gadolinium within the AP has not been explored further by histochemical analysis to date.

Moreover, it has not been investigated whether the T1 signal changes observed with MRI *in vivo* represent permanent deposition or long-term retention and whether, taking into account the total volume of GBCA injected, a drop of AP signal intensity can be detected after a certain amount of time.

Herein, we test the hypothesis that washout mechanisms from the AP gland occur after serial injections of gadodiamide and are a function of the cumulative injected volume and the post-injection time delay.

Materials and methods

This retrospective observational study was performed in accordance with the Declaration of Helsinki and was approved by the Institutional Ethical Committee of the University Campus Bio-Medico di Roma. The written informed consent for this specific study was waived by the aforementioned Committee. Based on our institutional policy, all patients signed the general agreement form to give their availability to the use of clinical and imaging data for research purposes.

Subjects. We screened our in-house image database and selected a time span from January 2008 to June 2017. We identified a group of 59 consecutive patients who had undergone at least 5 intravenous GBCAs injections, each exclusively with 0.1 mmol/kg body weight of Omniscan, GE Healthcare (gadodiamide 0.5 mmol/mL).

The exclusion criteria were: (1) empty sella; (2) previous neurosurgery; (3) abnormal renal function evaluated by calculating (Modification of Diet in Renal Disease study equation) the estimated glomerular filtration rate (GFR) from a blood sample obtained less than 3 months prior to the inclusion (GFR < 60 mL/min); (4) unsatisfactory images due to MR artifacts or absence of unenhanced sagittal T1 images; (5) presence of neoplastic lesions involving the pituitary gland.

MR imaging protocol. Imaging data were acquired at 1.5-T MRI system (MAGNETOM Avanto B13; Siemens, Erlangen, Germany), configured with a 12-element designed head matrix coil. The in-house MRI protocol includes the following sequences as previously described²⁴: axial FLAIR, coronal TSE T2- weighted with and without fat suppression, and sagittal two-dimensional (2D) TSE T1 weighted (TR 503 ms, TE 11 ms, matrix 256 × 256, FOV 25 cm², slice thickness 4 mm), conducted before and after intravenous administration of gadodiamide.

Based on the retrospective study design, small variations of MR parameters were allowed.

Image data analysis. The quantitative analysis of the relative signal intensity of the AP gland was conducted using a previously reported method²⁴.

Using a Carestream PACS workstation, the signal intensity of 5 random voxels was sampled in the AP on the mid-sagittal slice (including the pituitary stalk) of the unenhanced sagittal T1 images.

The mean signal intensity of the 5 voxels was taken as mean signal intensity of the AP. On the same slice an oval ROI of the central pons containing values of mean signal intensity was drawn.

Then, signal intensity ratios were calculated dividing the values of the AP by those of the pons obtaining AP-to-pons ratios.

All the measurements were performed at 4 timepoints: (1) at the first unenhanced MRI scan before any administration of gadodiamide (Baseline_Ratio); (2) at the MRI performed with the minimum post-injection time delay after the previous gadodiamide injection (Min_Delay_Ratio); (2) at the MRI performed with the maximum post-injection time delay after the previous gadodiamide injection (Max_Delay_Ratio); at the last available MRI scan for each subject (Last_Ratio). The last available brain MRI scan for each subject was the one performed at the greatest amount of previous gadodiamide cumulative doses until June 2017.

The ratios were compared between the first (Baseline_Ratio) and each individual timepoint (Min_Delay_Ratio, Max_Delay_Ratio and Last_Ratio) for all the subjects.

To correct for the different dose of injected gadodiamide at each timepoint and better clarify the potential effect of both time delay and total cumulative injection volume, we further divided the ratios obtained at the minimum and maximum post-injection time delay by the total volume of injected gadodiamide, to normalize the ratios (Norm_Min_Delay_Ratio and Norm_Max_Delay_Ratio), and adjust for the effect of the cumulative doses.

All the ROI drawings and image visual inspections were performed by consensus of two experienced neuro-radiologists (C. C. Q., 16 years of experience; C. A. M., 9 years of experience), who were blinded to any patients' information.

Statistical analysis. Descriptive statistics, means, ranges and standard deviations were assessed to understand central tendencies in each group. The normality of data distribution was tested using the Kolmogorov–Smirnov test. The differences between different ratios, obtained at variable timepoints, were explored by means of non-parametric Wilcoxon signed-rank test (2-sided p-value within 99% confidence interval).

The correlations were tested with non-parametric Spearman correlation coefficient.

Analyses were conducted by using the Statistical Package for the Social Sciences software package (version 24.0), setting the a priori significance level at $p < 0.05$.

	Minimum	Maximum	Mean (\pm standard deviation)
Age (years)	23	86	53 (14.68)
Minimum delay (days)	1	376	93 (87.93)
Maximum delay (days)	103	810	373 (208.89)
Last (days)	39	700	288 (191.59)
Doses minimum delay (N)	1	19	3.64 (3.57)
Doses maximum delay (N)	1	18	6.21 (3.72)
Doses last (N)	5	19	8.32 (3.80)
Volume minimum delay (mL)	10	266	51.08 (50.06)
Volume maximum delay (mL)	10	252	87.02 (52.08)
Baseline_Ratio	0.75	1.10	0.99 (0.07)
Min_Delay_Ratio	0.81	1.29	1.03 (0.09)
Max_Delay_Ratio	0.81	1.18	1.02 (0.09)
Last_Ratio	0.90	1.17	1.05 (0.06)
Norm_Min_Delay_Ratio	0	0.09	0.038 (0.027)
Norm_Max_Delay_Ratio	0	0.07	0.017 (0.014)

Table 1. Descriptive data of the included patients. The last MRI is intended as the one obtained after the greatest amount of previous gadodiamide cumulative doses. The maximum and minimum time delay MRIs are defined as those obtained respectively after the maximum and the minimum time lapse since the last gadodiamide injection regardless the amount of previous gadodiamide cumulative doses.

Results

Twenty-two patients were excluded from the analysis: 18 were affected by motion artifacts or pre-contrast sagittal T1-weighted images were missing, 3 were diagnosed with empty sella and 1 showed a metastatic lesion centered in the pituitary gland. Therefore, a group of 37 patients (15 males and 22 females) was finally considered for analysis.

Clinical indications to gadolinium-enhanced brain MRI for the patients was as follows: meningioma ($n=7$), optic neuritis ($n=1$), brain metastases ($n=14$), glioblastoma ($n=1$), multiple sclerosis ($n=10$), central nervous system lupus ($n=1$), arteriovenous malformation ($n=1$), hypertensive encephalopathy ($n=1$) and leukoencephalopathy ($n=1$).

Descriptive data of the variables collected for each patient and each timepoint are provided in Table 1.

As expected, there was a significant increase of AP T1 signal intensity in the Last_Ratio with respect to the Baseline_Ratio ($p<0.001$). A statistically significant result, albeit less strong, was also obtained with Min_Delay_Ratio ($p=0.003$) and Max_Delay_Ratio ($p=0.005$).

The comparison between Min_Delay_Ratio and Max_Delay_Ratio revealed absence of significant differences ($p=0.55$). However, by comparing normalized ratios, we found significantly higher values of Norm_Min_Delay_Ratio than Norm_Max_Delay_Ratio ($p<0.001$) (Fig. 1).

Moreover, all the normalized ratios taken together (Norm_Min_Delay_Ratio and Norm_Max_Delay_Ratio) demonstrated a statistically significant negative correlation with the post-injection time delay ($r = -0.31$; $p=0.006$) (Fig. 2).

Discussion

In this study, we found an increase of the signal intensity of AP on unenhanced T1 weighted MR images obtained at minimum as well as maximum post-injection time delay, in patients with normal renal function exposed to serial gadodiamide injections. The result confirms a previous report showing increased T1 signal intensity of the AP after chronic exposure to GBCAs²⁴.

The values calculated at minimum post-injection delay were not different than those obtained at maximum post-injection time delays. However, it should be taken into consideration that patients usually undergo MR imaging at shorter post-injection time delays early after the diagnosis of their disease and tend to have lower cumulative doses received, whereas the patients with longer post-injection time delays are those undergoing follow-up studies and, as long survivors, tend to have higher cumulative doses of gadolinium. Thus, to discriminate the effects of these two major variables potentially affecting the results (i.e. post-injection time delay and the cumulative volume of previous injected GBCAs), we normalized the signal intensity ratios by the volume of gadodiamide administered at the time of the measured ratio. Interestingly, we found a statistically significant difference between normalized ratios, as images obtained at minimum post-injection time delay showed higher signal intensity than those obtained at maximum post-injection delays and despite a lower cumulative injected volume of gadodiamide. This finding suggests that at least partial washout phenomena of retained/deposited gadolinium from the AP are influenced by the total injected volume and post-injection time delays. The significant negative correlation between normalized ratios and post-injection time delay reinforces this concept.

It is known that gadolinium colocalizes with other elements in tissues^{25–27}. Indeed, a colocalization between gadolinium and iron has been recently pointed out in some brain structures including DN and GP^{25–27}.

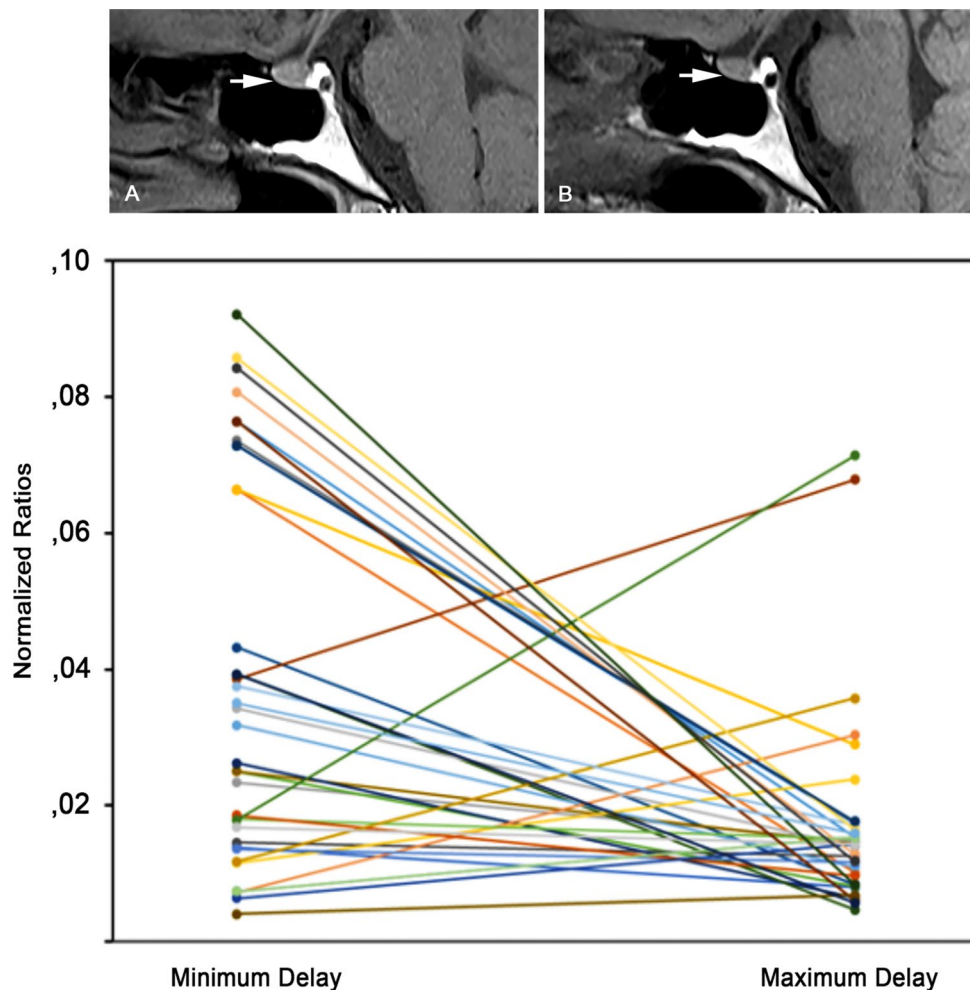


Figure 1. Sagittal unenhanced T1 MR images acquired after one previous gadodiamide injection with post-injection time delay of 1 day (A) and after four previous gadodiamide injections with post-injection time delay of 180 days (B). A slightly greater signal intensity of the anterior pituitary gland is visible in (A) with respect to (B) (arrows). The graph of the lower panel depicts a trend towards reduction of normalized ratios from minimum post-injection delay to maximum post-injection time delay. Each line represents one individual patient.

In patients with transfusion-related iron overload, such as those with β -thalassemia major or myelodysplasia, circulating iron first deposit in the reticuloendothelial system and subsequently in several parenchymal organs^{28,29}. In such cases, the intracranial structures more prone to iron deposition are those without blood–brain barrier such as pineal gland, choroid plexus, and pituitary gland^{28,29}. Thus, it is to be considered possible that gadolinium and iron might also colocalize within the AP.

The embryogenesis of the pituitary gland is complex. It originates from the joint of two distinct parts, the Rathke's pouch, which is formed as a dorsal evagination of the stomodeum, and the infundibulum, arising as a ventral extension of the diencephalon^{30,31}. With progression of the pituitary development, the cells of the anterior wall of Rathke's pouch proliferate fast in order to form the adenohypophysis. The growth of these cells produces two compartments (Atwell's fossae) that will be separated by a cellular median septum and initially filled with mesenchymal elements. The subsequent migration of mesenchymal elements from the fossae Atwell's fossae to the anterior surface of the infundibulum will eventually give rise to the blood vessels of the hypophyseal portal system^{30,32}. Of note, the AP is known to be the most vascularized among of all mammalian tissues, reached by about 0.8 mL/g/min of blood from the portal system^{30,33}. Moreover, the histology of the AP is characterized by interlacing cords of large polygonal cells separated by an extensive network of sinusoidal capillaries with fenestrated endothelium, in order to promote uptake of the secreted hormones^{30,34}.

Therefore, the rich vascular supply as well as the absence of blood–brain barrier and the fenestrated endothelium of sinusoidal capillaries make the pituitary gland a perfect site for a fast wash in and fast washout of elements traveling through the bloodstream.

Gadolinium deposition in tissues has been investigated by several groups in preclinical studies with mass spectrometry, histopathology and MR imaging but nobody focused on the AP to date^{21,35–37}.

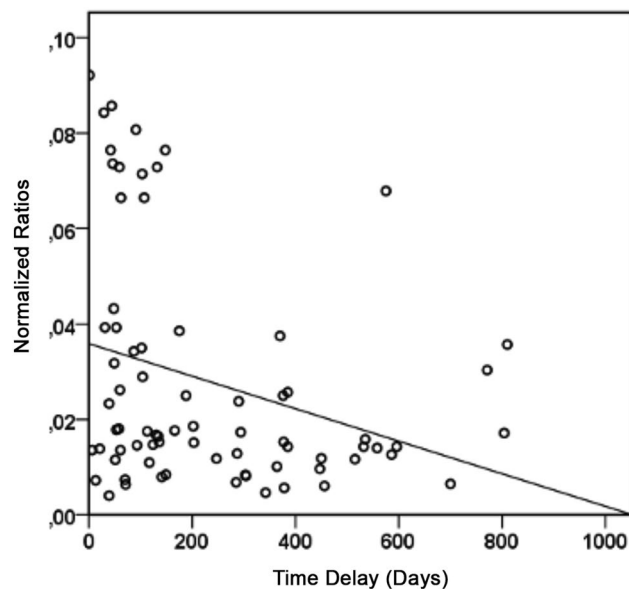


Figure 2. Scatterplot showing the significant negative association between normalized ratios and post-injection time delays.

Thus, the presence of gadolinium deposited within the AP has not been confirmed yet. On this respect, our results point towards gadolinium washout from the AP after a certain amount of time delay, suggesting retention rather than deposition; that is in keeping with the gross anatomy and histology of the AP. Since we found a significant increase of signal intensity on unenhanced T1 weighted images acquired at minimum as well as maximum post-injection time delays, a contribution of gadolinium deposition occurring at cellular and extra-cellular level within the AP cannot be ruled out.

Currently, the most accepted mechanism of gadolinium deposition after the i.v. injection of GBCA with linear structure such as gadodiamide is based on the entry into the brain through the cerebrospinal fluid and the glymphatic pathway and on the transmetallation with other elements showing high affinity for gadolinium-binding chelators^{38–41}. Therefore, the rich vascular supply of the AP might also not be critical in this context.

Indeed, the results reported in this study need to be further investigated and validated with analytical techniques on pre-clinical models.

This study has limitations that should be taken into account and might affect a generalization of the results. First, due to the retrospective nature of the study, we allowed small variations of the parameters of the standard MR imaging protocol. Second, the measurement of the AP signal intensity was performed on a single-slice sagittal T1-weighted 4 mm image; such a measurement is extremely difficult, is not performed on the entire volume of the AP and is greatly affected by images artifacts even if small. Third, the high T1 signal intensity is non-specific and is not restricted to gadolinium but occurs with many other paramagnetic substances. Fourth, it was not possible to consistently retrieve laboratory data about hormonal status of the patients.

Conclusions

We found a significant increase of T1 signal intensity on images obtained at minimum post-injection time delay as compared to those at maximum post-injection time delay. This result and the negative correlation between normalized ratios and post-injection time delays suggest at least partial washout phenomena of retained/deposited gadolinium from the AP that are influenced by the total injected volume and post-injection time delay.

Received: 27 March 2020; Accepted: 20 August 2020

Published online: 11 September 2020

References

- Perez-Castro, C., Renner, U., Haedo, M. R., Stalla, G. K. & Arzt, E. Cellular and molecular specificity of pituitary gland physiology. *Physiol. Rev.* **92**, 1–38 (2012).
- Parizel, P. M. *et al.* Gadolinium-DOTA enhanced MR imaging of intracranial lesions. *J. Comput. Assist. Tomogr.* **13**, 378–385 (1989).
- Palasz, A. & Czekaj, P. Toxicological and cytophysiological aspects of lanthanides action. *Acta Biochim. Pol.* **47**, 1107–1114 (2000).
- Kanda, T., Matsuda, M., Oba, H., Toyoda, K. & Furui, S. Gadolinium deposition after contrast-enhanced MR imaging. *Radiology* **277**, 924–925 (2015).
- Mallio, C. A., Quattrocchi, C. C., Rovira, À & Parizel, P. M. Gadolinium deposition safety: Seeking the patient's perspective. *AJNR Am. J. Neuroradiol.* **41**, 944–946 (2020).
- McDonald, R. J. *et al.* Gadolinium deposition in human brain tissues after contrast-enhanced MR imaging in adult patients without intracranial abnormalities. *Radiology* **285**, 546–554 (2017).
- Mallio, C. A., Rovira, À, Parizel, P. M. & Quattrocchi, C. C. Exposure to gadolinium and neurotoxicity: current status of preclinical and clinical studies. *Neuroradiology* **62**, 925–934 (2020).

8. Quattrocchi, C. C., Mallio, C. A., Errante, Y. & Beomonte Zobel, B. High T1 signal intensity in dentate nucleus after multiple injections of linear gadolinium chelates. *Radiology* **276**, 616–617 (2015).
9. Mallio, C. A., Ramalho, J. & Quattrocchi, C. C. Impact of brain irradiation, chemotherapy, and presence of primary brain tumors on changes in signal intensity after exposure to gadolinium-based contrast agents. *Radiology* **290**, 575–576 (2019).
10. Radbruch, A. *et al.* High-signal intensity in the dentate nucleus and globus pallidus on unenhanced T1-weighted images: Evaluation of the macrocyclic gadolinium-based contrast agent gadobutrol. *Invest. Radiol.* **50**, 805–810 (2015).
11. Parillo, M. *et al.* A structured survey on adverse events occurring within 24 hours after intravenous exposure to gadodiamide or gadoterate meglumine: A controlled prospective comparison study. *Invest. Radiol.* **54**, 191–197 (2019).
12. Quattrocchi, C. C. *et al.* Effect of age on high T1 signal intensity of the dentate nucleus and globus pallidus in a large population exposed to gadodiamide. *Invest. Radiol.* **53**, 214–222 (2018).
13. Guo, B. J., Yang, Z. L., Zhang, L. J. Gadolinium deposition in brain: Current scientific evidence and future perspectives. *Front. Mol. Neurosci.* **20**(11), 335 (2018).
14. Choi, J. W. & Moon, W. J. Gadolinium deposition in the brain: Current updates. *Korean J. Radiol.* **20**, 134–147 (2019).
15. Eisele, P. *et al.* Sodium MRI of T1 high signal intensity in the dentate nucleus due to gadolinium deposition in multiple sclerosis. *J. Neuroimaging.* **27**, 372–375 (2017).
16. Eisele, P. *et al.* Diffusion-weighted imaging of the dentate nucleus after repeated application of gadolinium-based contrast agents in multiple sclerosis. *Magn. Reson. Imaging.* **58**, 1–5 (2019).
17. Mallio, C. A. *et al.* Absence of dentate nucleus resting-state functional connectivity changes in nonneurological patients with gadolinium-related hyperintensity on T1-weighted images. *J. Magn. Reson. Imaging.* **50**, 445–455 (2019).
18. Zivadinov, R. *et al.* Cumulative gadodiamide administration leads to brain gadolinium deposition in early MS. *Neurology.* **93**, e611–e623 (2019).
19. Vymazal, J., Krámská, L., Brožová, H., Růžička, E. & Rulseh, A. M. Does serial administration of gadolinium-based contrast agents affect patient neurological and neuropsychological status? Fourteen-year follow-up of patients receiving more than fifty contrast administrations. *J. Magn. Reson. Imaging.* **51**, 1912–1913 (2020).
20. Mallio, C. A. *et al.* Within-network brain connectivity in Crohn's disease patients with gadolinium deposition in the cerebellum. *Neuroradiology* **62**, 833–841 (2020).
21. Mallio, C. A., Parillo, M., Zobel, B. B., Parizel, P. M., Quattrocchi, C. C. Effect of exposure to gadodiamide and brain irradiation on T1-weighted images and ADC maps of the dentate nucleus. *J. Magn. Reson. Imaging.* <https://doi.org/10.1002/jmri.27198> (2020).
22. Lohrke, J. *et al.* Histology and gadolinium distribution in the rodent brain after the administration of cumulative high doses of linear and macrocyclic gadolinium-based contrast agents. *Invest. Radiol.* **52**, 324–333 (2017).
23. Fingerhut, S. *et al.* Gadolinium-based contrast agents induce gadolinium deposits in cerebral vessel walls, while the neuropil is not affected: An autopsy study. *Acta Neuropathol.* **136**, 127–138 (2018).
24. Mallio, C. A. *et al.* Increased T1 signal intensity of the anterior pituitary gland on unenhanced magnetic resonance images after chronic exposure to gadodiamide. *Invest. Radiol.* **55**, 25–29 (2020).
25. El-Khatib, A. H. *et al.* Gadolinium in human brain sections and colocalization with other elements. *Neurology: Neuroimmunol. NeuroInflamm.* **6**, e515 (2019).
26. Radbruch, A. *et al.* Gadolinium deposition in the brain in a large animal model: Comparison of linear and macrocyclic gadolinium-based contrast agents. *Invest. Radiol.* **54**, 531–536 (2019).
27. Minaeva, O. *et al.* Nonhomogeneous gadolinium retention in the cerebral cortex after intravenous administration of gadolinium-based contrast agent in rats and humans. *Radiology* **294**, 377–385 (2020).
28. Çetinçakmak, M. G. *et al.* MRI-based evaluation of the factors leading to pituitary iron overload in patients with thalassemia major. *J. Neuroradiol.* **43**, 297–302 (2016).
29. Christoforidis, A. *et al.* MRI for the determination of pituitary iron overload in children and young adults with β -thalassaemia major. *Eur. J. Radiol.* **62**, 138–142 (2007).
30. Amar, A. P. & Weiss, M. H. Pituitary anatomy and physiology. *Neurosurg. Clin. N. Am.* **14**, 11–23 (2003).
31. Sadler, T. *Langman's Medical Embryology*. 8th edn. (Lippincott Williams & Wilkins, Philadelphia, 2000).
32. Allen, M. B. *The Pituitary: A Current Review* (ed. Allen, M. B.) (Academic Press, New York, 1977).
33. Aron, D., Findling, J., Tyrell, J. *Basic and Clinical Endocrinology*. 5th edn. (Appleton and Lange, Stamford, 1997).
34. Tuchmann-Duplessis, H., Auroux, M., Haegel, P. *Illustrated Human Embryology*, Vol. III. (Springer, New York, 1977).
35. Robert, P. *et al.* T1-weighted hypersignal in the deep cerebellar nuclei after repeated administrations of gadolinium-based contrast agents in healthy rats: Difference between linear and macrocyclic agents. *Invest. Radiol.* **50**, 473–480 (2015).
36. Robert, P. *et al.* Linear gadolinium-based contrast agents are associated with brain gadolinium retention in healthy rats. *Invest. Radiol.* **51**, 73–82 (2016).
37. Boyken, J., Frenzel, T., Lohrke, J., Jost, G. & Pietsch, H. Gadolinium accumulation in the deep cerebellar nuclei and globus pallidus after exposure to linear but not macrocyclic gadolinium-based contrast agents in a retrospective pig study with high similarity to clinical conditions. *Invest. Radiol.* **53**, 278–285 (2018).
38. Taoka, T. & Naganawa, S. Gadolinium-based contrast media, cerebrospinal fluid and the glymphatic system: Possible mechanisms for the deposition of gadolinium in the brain. *Magn. Reson. Med. Sci.* **17**, 111–119 (2018).
39. Deike-Hofmann, K. *et al.* Glymphatic pathway of gadolinium-based contrast agents through the brain: Overlooked and misinterpreted. *Invest. Radiol.* **54**, 229–237 (2019).
40. Jost, G. *et al.* Penetration and distribution of gadolinium-based contrast agents into the cerebrospinal fluid in healthy rats: A potential pathway of entry into the brain tissue. *Eur. Radiol.* **27**, 2877–2885 (2017).
41. Aime, S. & Caravan, P. Biodistribution of gadolinium-based contrast agents, including gadolinium deposition. *J. Magn. Reson. Imaging.* **30**, 1259–1267 (2009).

Author contributions

All the authors made substantial contributions to all the categories established by the International Committee of Medical Journal Editors (ICMJE) guidelines on authorship: (1) C.A.M.: conception and design, acquisition of data, analysis and interpretation of data; drafting the article and revising it critically for important intellectual content; final approval of the version to be published; agreement to be accountable for all aspects of the work in ensuring that questions related to the accuracy or integrity of any part of the work are appropriately investigated and resolved. (2) L.M.: analysis and interpretation of data; drafting the article and revising it critically for important intellectual content; final approval of the version to be published; agreement to be accountable for all aspects of the work in ensuring that questions related to the accuracy or integrity of any part of the work are appropriately investigated and resolved. (3) M.P.: analysis and interpretation of data; drafting the article and revising it critically for important intellectual content; final approval of the version to be published; agreement to be accountable for all aspects of the work in ensuring that questions related to the accuracy or integrity of any part of the work are appropriately investigated and resolved. (4) G.L.V.: analysis and interpretation of data;

drafting the article and revising it critically for important intellectual content; final approval of the version to be published; agreement to be accountable for all aspects of the work in ensuring that questions related to the accuracy or integrity of any part of the work are appropriately investigated and resolved. (5) B.B.Z.: analysis and interpretation of data; drafting the article and revising it critically for important intellectual content; final approval of the version to be published; agreement to be accountable for all aspects of the work in ensuring that questions related to the accuracy or integrity of any part of the work are appropriately investigated and resolved. (6) P.M.P.: analysis and interpretation of data; drafting the article and revising it critically for important intellectual content; final approval of the version to be published; agreement to be accountable for all aspects of the work in ensuring that questions related to the accuracy or integrity of any part of the work are appropriately investigated and resolved. (7) C.C.Q.: conception and design, acquisition of data, analysis and interpretation of data; drafting the article and revising it critically for important intellectual content; final approval of the version to be published; agreement to be accountable for all aspects of the work in ensuring that questions related to the accuracy or integrity of any part of the work are appropriately investigated and resolved.

Funding

None.

Competing interests

The authors declare no competing interests.

Additional information

Correspondence and requests for materials should be addressed to C.A.M.

Reprints and permissions information is available at www.nature.com/reprints.

Publisher's note Springer Nature remains neutral with regard to jurisdictional claims in published maps and institutional affiliations.



Open Access This article is licensed under a Creative Commons Attribution 4.0 International License, which permits use, sharing, adaptation, distribution and reproduction in any medium or format, as long as you give appropriate credit to the original author(s) and the source, provide a link to the Creative Commons licence, and indicate if changes were made. The images or other third party material in this article are included in the article's Creative Commons licence, unless indicated otherwise in a credit line to the material. If material is not included in the article's Creative Commons licence and your intended use is not permitted by statutory regulation or exceeds the permitted use, you will need to obtain permission directly from the copyright holder. To view a copy of this licence, visit <http://creativecommons.org/licenses/by/4.0/>.

© The Author(s) 2020